Available online at www.CivileJournal.org

Civil Engineering Journal

Vol. 4, No. 7, July, 2018

Updated Probabilistic Seismic Hazard Assessment for Iraq/2018

Mustafa Shakir Farman [a,b*], AbdulMuttalib Isa Said [c]

[a] *Faculty Member, Technical Institute of Samawa, Al-Furat Al-Awsat University, Iraq.*

[b] *Ph.D. student, Civil Engineering Department, University of Baghdad, Baghdad, Iraq.*

[c] *Prof., Faculty Member, Civil Engineering Department, University of Baghdad, Baghdad, Iraq.*

Received 25 April 2018; Accepted 12 July 2018

Abstract

Recently, Iraq has experienced an unprecedented seismic activity, specifically, near the east boundary with Iran which reveals the need to re-evaluate the seismic hazard at this region. This study consists of two phases. The first is collecting the earthquake records covering the recent events till the end of November 2017 including the 12 November 2017 (7.3Mw) earthquake, and applying data processing to get the net data for independent events for the study area which were more than 4300 of net main earthquakes of Mw $\geqslant$ 4 and were used in the second phase. The second phase is applying the PSHA method by dividing the study area into a grid of small cells of size 0.5×0.5° and the hazard parameters were calculated at the center of each of these grid cells then, converting the final results to contours over the study area. It is found that the values increases towards the east-northeast and north due to the continued tectonic boundary convergence between the Arabian, Iranian and Turkish plates which produces intense earthquake activity. The design spectral acceleration at 0.2 and 1.0 seconds found to be 0.33, 0.17, 0.47, 0.25, 0.71, 0.35 g for Basra, Baghdad and Erbil, respectively. The comparison between the PGA values from this study and from the seismic hazards maps from Iraqi seismic codes of 1989, 1997 and 2016, for return periods of 475 and 2475 years, reveals the continued increase with time which reveals the need to updating the seismic hazard maps continuously.

Keywords: PSHA; Iraq; Main Earthquakes; PGA; Spectral Accelerations; Seismic Hazard.

1. Introduction

Iraq situated on the north portion of the Arabian Plate and surrounded in the north and east boundaries by the Bitlis-Zagros Thrust and Fold Belt, where the convergent tectonic boundary between the Arabian and Eurasian plates produces intense earthquake activity. Figure 1.a shows the counterclockwise rotational motion and northeast trending transitional motion of the Arabian plate. Most of the earthquakes are occurring in the crust along the Taurus and Zagros mountain ranges and their foothills [1, 2].

The Arabian plate is subducted under the Iranian and Turkish plates compressing the Tethyesides geosyncline belt as part of the Alpine movement, which arrived its climax in the Tertiary and continued up to the Pliocene, where the Tethys Sea was totally closed in the region. Zagros Mountains that are part from the Alpine-Himalayan orogenic system can be subdivided into three structural zones which are: an inner crystalline zone of overthrusting, an imbricate zone, and a zone of folding that is referred to as the simply folded zone (the north and northeastern parts of Iraq, Figure 1.b). Taurus Mountains took an E-W trend in the north of Iraq. These two plate boundaries have complicated tectonic patterns, and it is believed that the forces which have formed these two plate boundaries are still active [3].

* Corresponding author: alishf2013@yahoo.com

http://dx.doi.org/10.28991/cej-0309199

At recent years, Iraq has experienced an unprecedented seismic activity, specifically, near the east boundary with Iran which reveals the need to re-evaluate the seismic hazard at this region. One of the main previous studies that went a long way in applying the PSHA for Iraq is reported by the seismic design code of Iraq (1988) where the Iraqi earthquakes data file has been compiled and prepared for the period 859 – 1986. Completeness analysis indicated that the data were completed for seismic events of Ms $\geqslant$ 4.8. Ten area sources were identified and used in the report. The activity parameters of these seismic sources have been evaluated. The final results have been plotted in the form of contours of PGA for return periods of 50, 100, 200 and 500 years. The attenuation relationships given by Donovan 1973a, McGuire 1977, Esteva 1974, Fahmi 1988 and Cornell 1979 for the PGA were used in conjunction with Poisson distribution in the PSHA to plot these map [4-8].

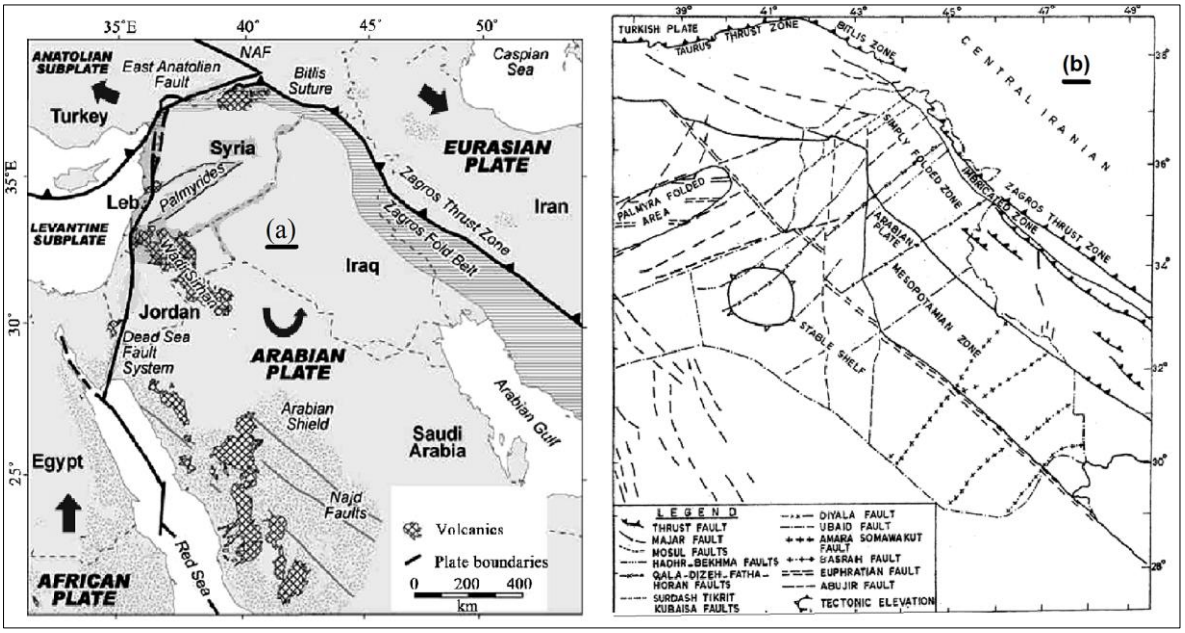

Figure 1. a) The tectonic setting of Iraq and environs, b) Main structural zones of Iraq [3]

Al-Sinawi et al. (2003) published their study on Iraq region that was executed a decade before their publication. They used earthquakes data for the period 1900-1988 to plot contour maps of PGA for Iraq region using return periods of 25, 50, 100 and 200 years. Five line sources and four seismic area sources were used in their study. They used an attenuation relationship given by Esteva 1974 in conjunction with Poisson distribution in the PSHA to plot these maps. They were found that the PGA increases towards the east-northeast and the east. The de-clustering process was not applied on the earthquakes data in the previous two studies, which means, their data includes dependent events whereas Poisson distribution is used for independent events [9].

Also, recent codes use a probability of exceedance of 2% in a 50 year period, which means, the return period is 2475 years, whereas the larger return period used in the previously mentioned two studies is 500 years. Also, the outputs of these two studies were in terms of the PGA, while the recent codes and researches used the spectral accelerations at 0.2 and 1.0 seconds as aground motion intensity measure.

Ameer et al. (2005) studied the seismicity of Iraq region using seismicity data that has been collected and prepared for the period 1905–2000. Completeness analysis indicated that the earthquakes data were completed for Ms≥4.8. Also, they found that the activity parameters a and b of the complete data for Iraq are 6.49 and 0.89, respectively. They proposed a seismic sources model for Iraq region that includes thirteen of area sources. The activity parameters of these sources have been evaluated, but their study not continued to include all the PSHA process [3]. Onur et al. (2016) studied the seismic activity of Iraq region which is the latest study till now. They used earthquake data that encompasses the region bounded by longitudes (36º –51º) E and latitudes (26º - 40º) N, and includes about 4,000 earthquakes of Mw≥ 4.0 for the period 1900-2009 and including dependent events. Completeness analysis indicated that the data were completed for Mw≥ 6.5. They used the geological and tectonics information to identify twelve area sources. The activity parameters a and b were evaluated for each of these sources using the developed catalogue whereas m_{max} values have been calculated using the geometry of known faults inside each source. Also, contour maps of PGA and spectral accelerations at 1.0 and 0.2 seconds have been plotted for a return period of 2475 years [2]. For the seismic sources in the active shallow crustal region, they used four attenuation relationships given by Boore et al. (2014), Chiou and Youngs (2014) and Campbell and Bozorgnia (2014) in conjunction with Poisson distribution in the PSHA to plot these maps, but they based on dependent data events. Also, they are divided the data of the study area into three main regions based on a detailed analysis, these are the stable, Bitlis and Zagros regions. This is to capture the regional variability [10-12].

According to the previous prelude and the increasing seismic activity in the region, there is an urgent need to re-apply the probabilistic seismic hazard analysis (PSHA) in order to update the seismic hazard maps for Iraq but basing on earthquake data to be collected including the recent earthquakes till the end of November 2017 and including the 12 November 2017 (7.3Mw) earthquake, and after applying data processing to get the net earthquakes catalogue of independent events, which is the main objective of this study.

Accordingly, this study can be divided into two main stages, the first is collecting earthquakes data records and applying data processing including homogenization, removing duplication, de-clustering and completeness analysis. The second stage is applying all steps of the PSHA method based on the resulted data from the first stage.

2. Collecting and Processing Data

The earthquakes data prepared for this study covers an area outlined by longitudes (36º.00 –51º.00) E and latitudes (26º.00 - 40º.00) N, which is the same area used by Onur et al. (2016), and their outlines are about 300 km distance to nearest boundary of Iraq [2]. Four main sources used in compiling these data, the first one is the Iraqi earthquakes data file from the report of the seismic design code of Iraq (1988), that includes more than 600 earthquakes for the time period 859 – 1986, and they are in terms of Mb, ML, Ms. The second source is the Iranian earthquake data from Iranian Institute of Earthquake Engineering and Seismology (IIEES) that includes about 9500 of earthquakes for the period started from 1900 up to the end of November 2017, and they are in terms of Mb, ML, Mw, Ms, MD. The third source is the Turkish earthquake data from the Disaster and Emergency Management Authority of Turkey (AFAD) that includes more than 2300 of earthquakes for the period started from 1900 up to the end of November 2017 and they are in terms of Mb, ML, Mw, Ms. The fourth source is the global CMT catalog that contains 238 of earthquakes for the period started from 1976 up to the end of November 2017, and they are in terms of Mb, Mw and Ms.

Each of the four earthquakes data sources has its different and special tabulated format, therefore a MatLab program is constructed to read and deal and rearrange these different formats in a one unified tabulated format of location, date, time, moment magnitude scale and the hypocenter depth.

The Mw scale is a more accurate measure, specifically, for large earthquakes, besides that most of the contemporary attenuation relationships are in terms of Mw, therefore; all magnitude scales will be converted to Mw. In order to develop relationships between Mw and other magnitude scales, earthquakes data from the same study area are used. The data of the CMT catalogue provides Mb, Ms, and Mw magnitudes for individual earthquake events, hence; it is used to calibrate the relationships that converting Mw to Mb, (Figure 2), and Mw to Ms, (Figure 3).

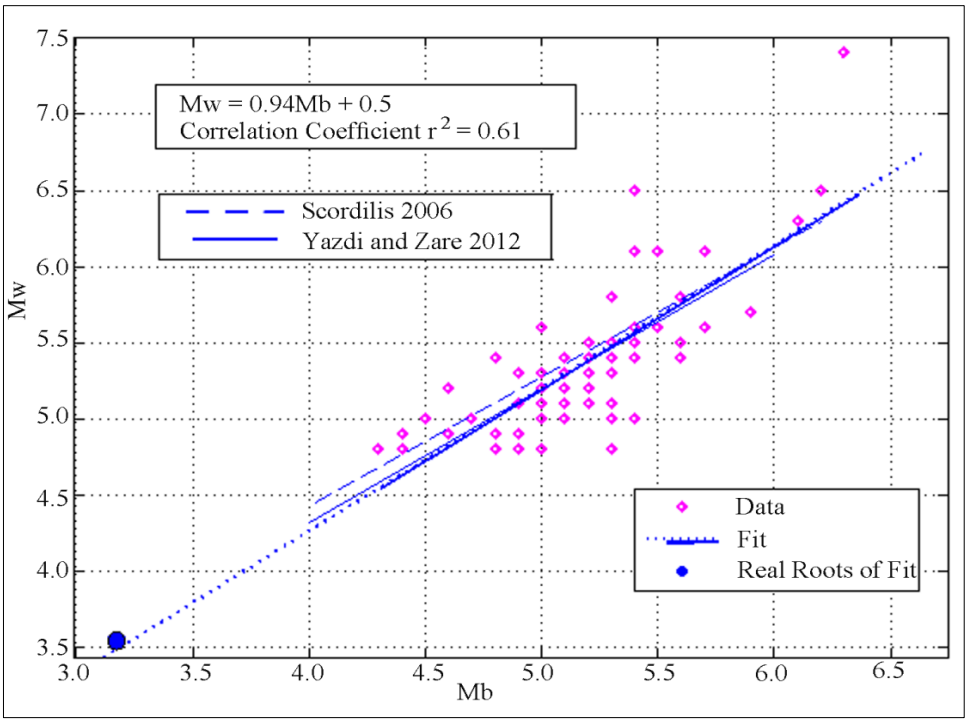

Figure 2. Regression relation between Mw and Mb

As can be seen from these figures that the resulted solid-line of regression of Mb to Mw in Figure 2 is near to line of Yazdi and Zare (2012) [12]. In Figure 3, the resulted solid-lines of regression of Ms to Mw are near to lines of Yazdi and Zare (2012) and lines of Scordilis (2006) [13, 14]. Figure 4 shows the resulted relation between Mw and ML. The

four Equations 1, 2a, 2b and 3 are formulated from relations of Figures 2, 3 and 4. The equation given by Onur et al. (2016), which is Equation 4, is used directly to convert MD to Mw, this is due to the few events in terms of MD.

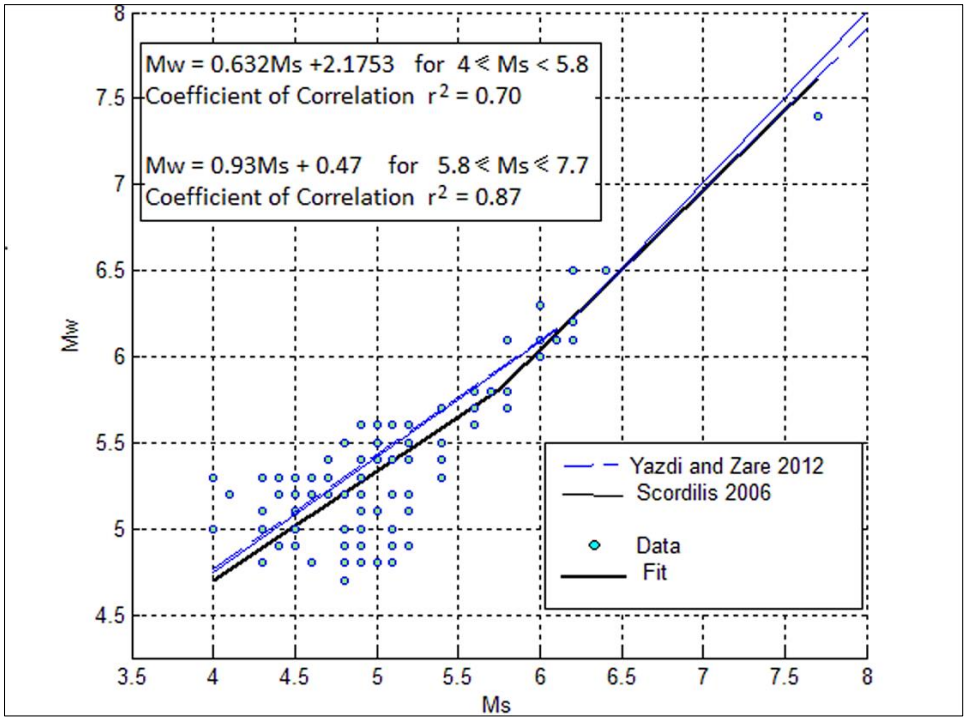

Figure 3. Regression relation between Mw and Ms

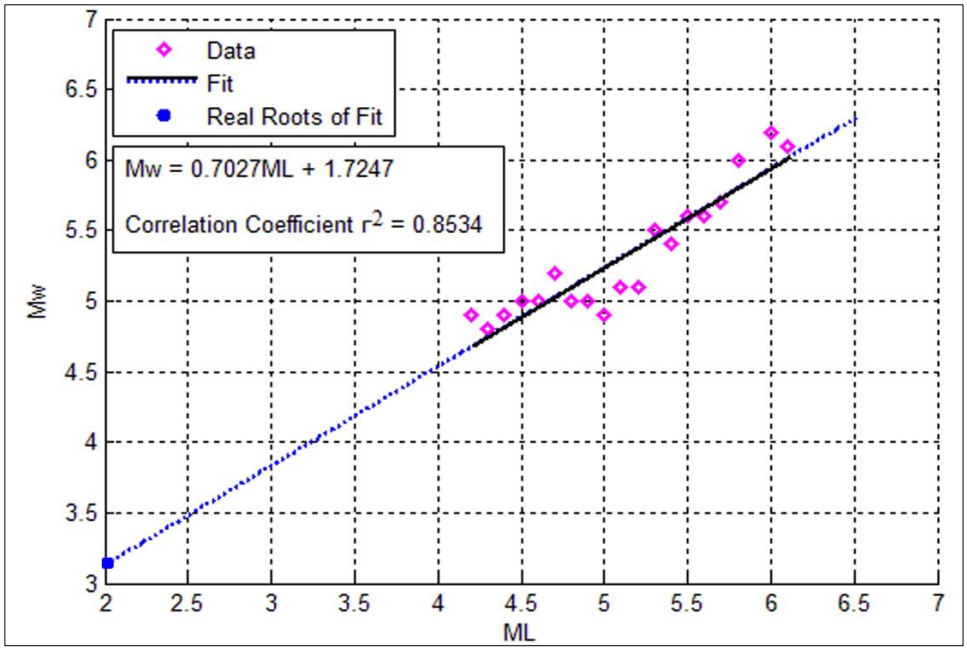

Figure 4. Regression relation between Mw and Ml

$$Mw = 0.94Mb + 0.50 \quad \text{for} \quad 4.2 \leq Mb \leq 6.4 \tag{1}$$

$$Mw = 0.632Ms + 2.1753 \quad \text{for} \quad 4 \leq Ms < 5.8 \tag{2a}$$

$$Mw = 0.93Ms + 0.47 \quad \text{for} \quad 5.8 \leq Ms \leq 7.7 \tag{2b}$$

$$Mw = 0.7027Ml + 1.7247 \quad \text{for} \quad 4.2 \leq Ml \leq 6.2 \tag{3}$$

$$Mw = 1.067MD + 0.1758 \quad \text{for} \quad 3.0 \leq MD \leq 5.0 \tag{4}$$

Combining the four earthquakes data sets led to some duplicate events, that have to be removed. Wheeler (2003) considered the earthquakes data are duplicated when their similarity in time are within one day, ten hours, 60 minutes and one minute for those that before 1800, 1900, 1950 and during or after 1950, respectively. He based on the fact that the time windows are larger for older earthquakes because reporting was often slower and time keeping may have been less accurate. Also, he considered similarity in magnitude within a few tenths of a magnitude unit, and similarity in location within a few tenths of degree are duplication [15]. Nasir et al. (2013) considered similarity in location within 0.05 degree and similarity in time within one hour are duplication [16].

The criteria of Nasir (2013) will be used in this study but with the time windows from the criteria of Wheeler (2003). A MatLab program is constructed to read the combined data and to remove duplicated events basing on the above selected criteria. After combining seismic events of Mw≥4 from the four data sets, the total number of events in the combined catalogue reached to 7415. The duplicated events were 461, therefore; the resulted net catalogue contains 6954 of events [15, 16].

Windowing procedures are the simple ways of identifying and removing aftershocks to get the main independent shocks, (de-clustering), basing on the general assumption that seismic events are Poissonian distributed. Gardner and Knopoff (1974) proposed a broad windowing procedure for time and distance in terms of magnitude and presented in a table. The windowing algorithm given by Uhrhammer (1986) is easy to implement, straight forward and presented in two equations for time and distance, [17-20].

The windowing algorithm given by Uhrhammer (1986) will be used in this study to remove the aftershocks and foreshocks, (dependent events). A MatLab program is constructed to read the net catalog of unduplicated earthquakes and to apply the de-clustering process based on the algorithm given by Uhrhammer (1986). The net catalogue contains 6954 events, and remain only 4315 main events after de-clustering. That means, about 38% of the total net events have been removed by de-clustering process, Figure 5. Also, it is found that about 91% of the main shocks have a depth ranging 0 to 35 km, which indicates that most of earthquakes in the Iraq region exhibit shallow crustal seismic activity. These main earthquake events and their information will be considered as the input data file for the *PSHA* analysis.

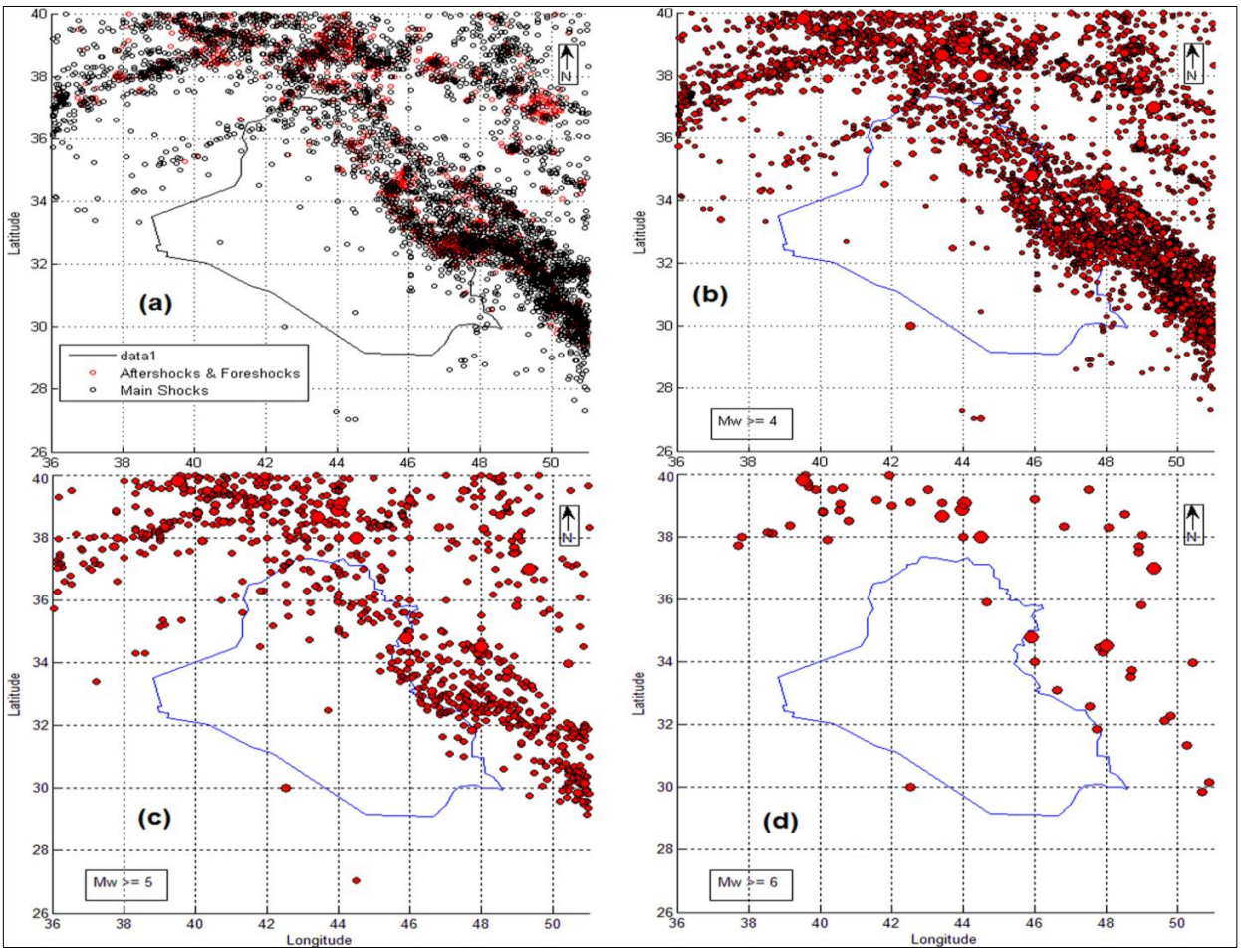

Figure 5. a) Epicentral distribution for the total 6838 shocks with Mw>= 4, red circles are the 2639 aftershocks and foreshocks, black circles are the 4315 main shocks which are same as that in drawing (b), b) main shocks with Mw>= 4, c) main shocks with Mw>= 5, d) main shocks with Mw>= 6

Several methods have been proposed to identify the magnitude, (Mc), at and above which an earthquake data file can be considered to be completed, or to identify time intervals within which a certain magnitude range of the data file can be considered to be completely reported. Stepp (1972) proposed a statistical and graphical method which is used to identify completeness time intervals of the reported magnitudes [21].

One of the mathematical methods used to estimate completeness magnitude is the FMD method. In this method, Mc is identified as the magnitude at and above which 90% of earthquakes data can be modeled by the Gutenberg and Richter (GR) law and it is called the Goodness of Fit method, Wiemer, S., Wyss, M. (2000), [22]. The Gutenberg and Richter (1944) law can be written as, (Baker 2008) [23, 24]:

$$\text{Log } N_m = a - b.m \tag{5}$$

Where a and b are constants to be obtained by regression of past earthquakes data, N_m is the annual rate of earthquakes with magnitudes greater than *m*.

In this method, a and b values of the GR law as a function of the minimum magnitude, (Mci), are computed, based on the events with $M \geq Mci$. The b and a values are estimated using the maximum likelihood estimate. Next, a synthetic distribution of magnitudes using the same a, b and Mci values is computed. This distribution represents a perfect fit to GR law. Then, the goodness of fit, R, is computed as, [22]:

$$R(a, b, Mci) = 100\left(1 - \frac{\sum_{Mci}^{Mmax} |\beta i - \gamma i|}{\sum_i \beta i}\right) \tag{6}$$

Where: γi is the predicted cumulative number of earthquake events while βi is the observed cumulative number of earthquake events, both in each magnitude bin. The synthetic distribution based on GR law will not model the FMD adequately if Mci is smaller than the right Mc. That means, the goodness of fit (R) that computed in percent of total number of observed earthquake events, is poor. R increases with increasing Mci until reaches a maximum value. At this Mci, the GR law with the estimated a and b values can explain R% of the data variability and beyond this Mci, R may decrease gradually, but, Mc is defined as the value of Mci at which the GR law can model 90% or more of the FMD, [22].

The analysis of completeness was performed on the de-clustered catalogue for the whole study area and for each seismic source using the goodness of fit method that was converted into a MatLab program based on Equation 6. It is found that the earthquakes data of the de-clustered catalogue are complete for Mw≥5.4 since 1900 where b=1.1114 and a=6.4143, as shown in Figure 6.A. In Figure 6.b, the result of completeness analysis for source zone 7 is presented as an example for seismic sources. Also, the Stepp method is applied on the de-clustered catalogue to identify the completeness intervals, which are found to be: 5.5<=Mw<6 are complete since 1900, 5.0<=Mw< 5.5 are complete since 1928, 4.5<=Mw< 5 are complete since 1968 and 4.0<=Mw< 4.5 are complete since 1988, Figure 7.A. The recurrences of the previous intervals have been extrapolated along the total period and then fitted to GR law as shown in Figure 7.B, where b=1.1327 and a=6.5681, which are near to that of Goodness of fit in Figure 7.A. It is necessary to mention that all the programs used in processing the data have been checked manually.

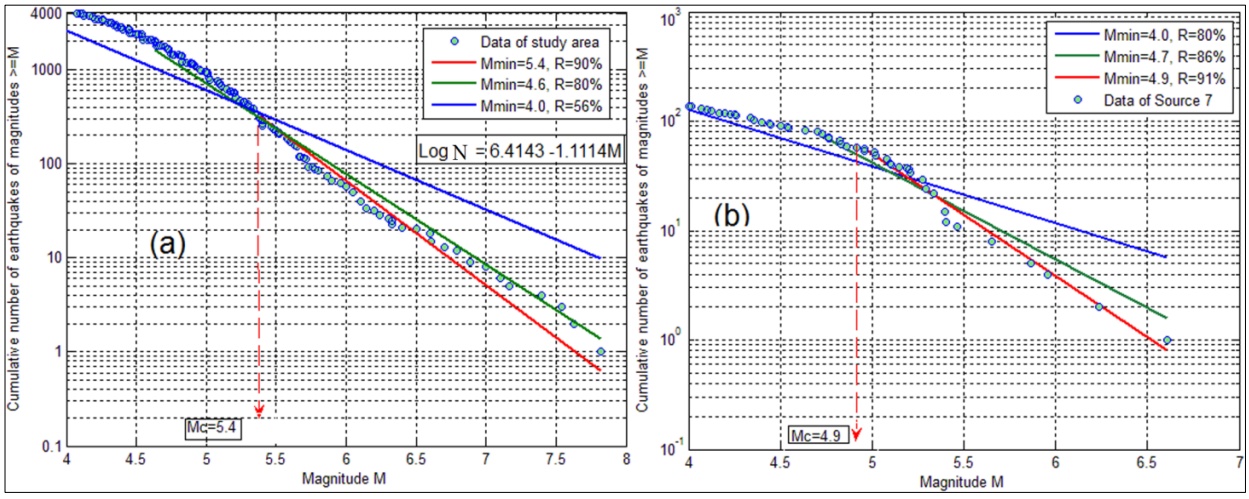

Figure 6. Applying completeness using Goodness of fit for: a) the whole study area, b) Source 7

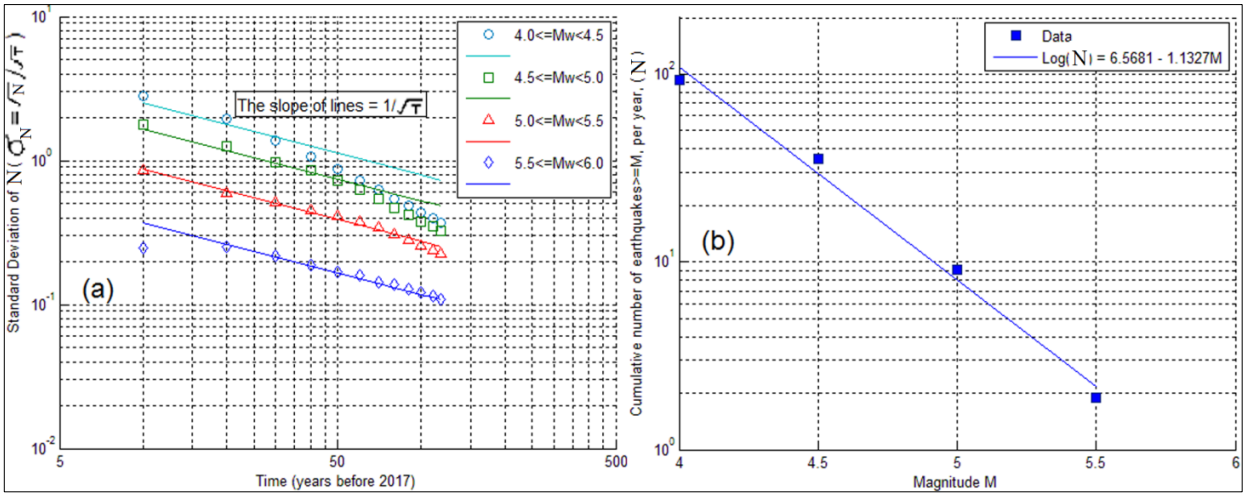

Figure 7. Applying completeness for the study area using Stepp method: a) Completeness intervals, b) Fitting to Gutenberg - Richter (1944) law

3. The PSHA Formulation

The seismic hazard at a site is generally defined by the seismicity intensity measure, IM. Formulation of the PSHA is generally concerned with the estimation of the expected occurrence rate, N (IM > z), for the seismicity intensity measure, IM, to exceed a specified value, z. For this purpose and based on the original formulation of Cornell (1968) and that of Kramer (1996) [26, 27], this rate is formulated in the following Equation [24, 27]:

$$N(IM > z) = \sum_{i=1}^{n_{sources}} N_m\,(Mi > m_{min}) \sum_{j=1}^{n_M} \sum_{k=1}^{n_R} P(IM > z|m_j, r_{ek}) P(M_i = m_j)\, P(R_i = r_{ek}) \quad (7)$$

Where: $P(IM > z|m_j, r_{ek})$ is computed based on the ground motion prediction equation, (GMPE), where the GMPEs give the intensity measure of ground motion in terms of its mean logarithm, $(\widehat{\text{Log IM}})$, and by using the normal distribution:

$$P(IM > z|m_j, r_{ek}) = 1 - \phi\left[\frac{Logz - \widehat{\text{Log IM}}}{\sigma_{LogIM}}\right] \quad (8)$$

Where: σ_{LogIM} is the standard deviation provided by the GMPE, $P(M_i = m_j)$ and $P(R_i = r_{ek})$ are the discretized probabilities of occurrences for magnitude and distance. The conditional probabilities of exceedance of all possible distances and magnitudes are added up through the summation operations. It is clear from Equation 7 that each conditional probability of exceedance is weighted with the probability of occurrence of the related magnitude and distance.

n_R and n_M: are numbers of the discretized range of possible distances, Ri, and magnitudes, Mi, respectively, for each source i.

$N_m(Mi > m_{min})$: is the rate of occurrence of earthquakes with magnitudes greater than the minimum magnitude, m_{min}, for each seismic source i and it is computed from Equation 5.

Earthquakes with magnitudes less than m_{min} are of little engineering importance, therefore, they will not be considered in the computations, (Baker 2008). Mostly, there will be more than one source. Hence, the rate of $(IM > x)$ from all sources are computed from the sum of rates of $(IM > x)$ produced from each source.

The area seismic sources will be subdivided into small-size elements. Then, the epicenter of each small element will be considered to be lying at the geometric center point of that element [28].

The points for the geometric centers of the small elements will form a regular grid of nodes. All nodes of this grid are equally spaced in both longitude and latitude. Each node location is defined by one geographic coordinate which are (longitude, latitude). All nodes contained inside the polygon of an area source represent, in a discrete way, this area source. The spacing (in km) between any two contiguous nodes adjacent to the equator is greater than that at higher latitudes. That means, the shape of elements tends to be squeezed as moving downward or upward towards the poles [28].

Accordingly, an easy method is adopted to assure the homogeneity of the distribution of seismicity. In this method, the seismicity is distributed in proportional to the element size. Particularly, for the seismic activity of each source to be

uniformly distributed, each of the epicentral locations of the small elements is assigned a weight in proportion to their areas, and based on the following relationship, [28, 29]:

$$P(R_i = r_{ek}) = \frac{Ae_k}{A_{src}} \quad (9)$$

Where: Ae_k is the area of a small element k, and computed by the following relationship:

$$Ae_k = 4\pi.spc^2.\left[\frac{\text{earth radius}}{360}\right]^2 \cos(\text{Latitudeofelement center}) \quad (10)$$

Where: spc is the distance in degrees between each two neighboring grid nodes used to discretize the seismic area source. Earth radius is the mean radius of Earth and it is equals to 6371 km, [28] and $\mathbf{A_{src}}$ is the total source area which is computed by summation of areas of all elements of the source. The element-to-site distance, r_{ek}, is computed by using the spherical law of cosines, which is:

$$r_{ek} = \left(\frac{\pi}{180}\right).\text{earth radius}.\cos^{-1}(\sin(Lat1).\sin(Lat2) + \cos(Lat1).\cos(Lat2).\cos(long2 - long1)) \quad (11)$$

Based on Equation 5, the cumulative distribution function for magnitudes of source i is, [24, 27]:

$$F_{Mi}(mi) = \frac{1 - 10^{-b(mi - mi_{min})}}{1 - 10^{-b(mi_{max} - mi_{min})}}, \qquad \text{where; } mi_{min} < mi < mi_{max} \quad (12)$$

Where: mi_{max} is the maximum earthquake magnitude that can be produced by a given source i. Finally:

$$P(M_i = m_j) = F_{M_i}(m_{j+1}) - F_{M_i}(m_j) \quad (13)$$

Where: mj are the discrete domain of earthquake magnitudes, arranged in such a way that mj<mj+1=mj +dm. Referring to Equation 13, the probabilities of all magnitudes between the values mj and mj+1 are assigned to the discrete value mj. This approximate procedure will not affect numerical results as much as the discrete magnitudes become closely spaced. Therefore, the practical PSHA analysis mostly uses a magnitude spacing, (dm), equals or less than 0.1 [24].

4. Earthquake Occurrences with Time

In accordance with Poisson's assumption, the probability that the ground motion intensity exceeds the test level z at least once during a specified time interval t will be computed as [27]:

$$P(IM > z) = 1 - e^{-N.t} \quad (14)$$

It is well mentioning that rate N in Equation 14 is the same as $N(IM > z)$ from Equation 7, therefore Equations 7 and 14 as will be noticed later are used in conjunction.

5. Formulation of the PSHA Steps on Iraq

After the data has become ready, a number of subroutines have been built and connected together using MatLab in order to apply the PSHA method. Each subroutine executes one of the steps of PSHA. Then, a main program has been built just to call these subroutines to execute the whole PSHA steps in a sequential manner according to the sequence of these steps. It is well mentioning that this program will be checked by testing its results with another work at end of Section (5.5).

5.1. Identifying Seismic Sources

The twelve area sources with a uniform seismicity rates that identified and used by Onur et al (2016) will be adopted and used in this study since they cover most area of Iraq and its surrounding regions and their events. Accordingly, Figure 8 shows the spatial distribution of the adopted seismic source model besides the epicentral locations of earthquakes data of the final net catalog [2].

In reference to Figure 8, most of the data are inside the sources lying along the border region with Turkey and Iran, i.e. in the active shallow crustal region. Also, the method used to identify each area source is illustrated in Figure 9, where (x_o, y_o), (x_f, y_f): are the coordinates, (in degrees), of the lower left point and the upper right point of the study area and then, the data will be distributed to these specified sources according to their coordinates. Finally, the output will be the data and its number for each source.

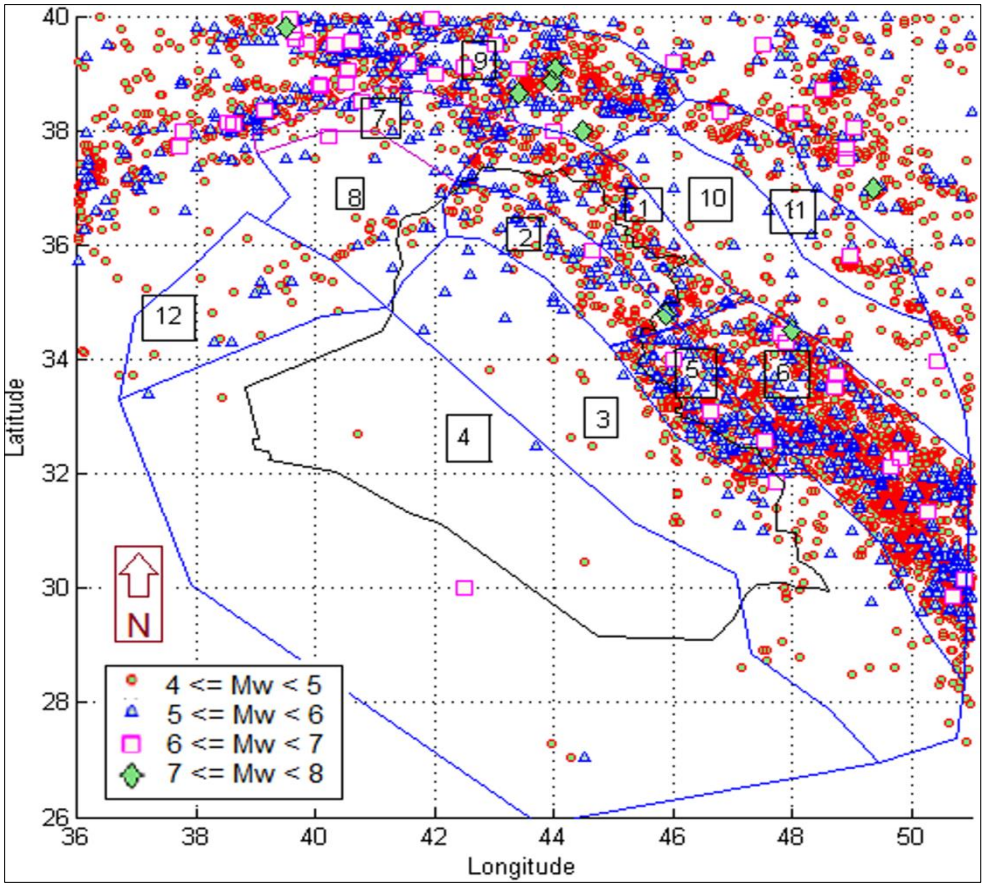

Figure 8. The used seismic source model and epicentral locations of earthquakes of the final net catalogue

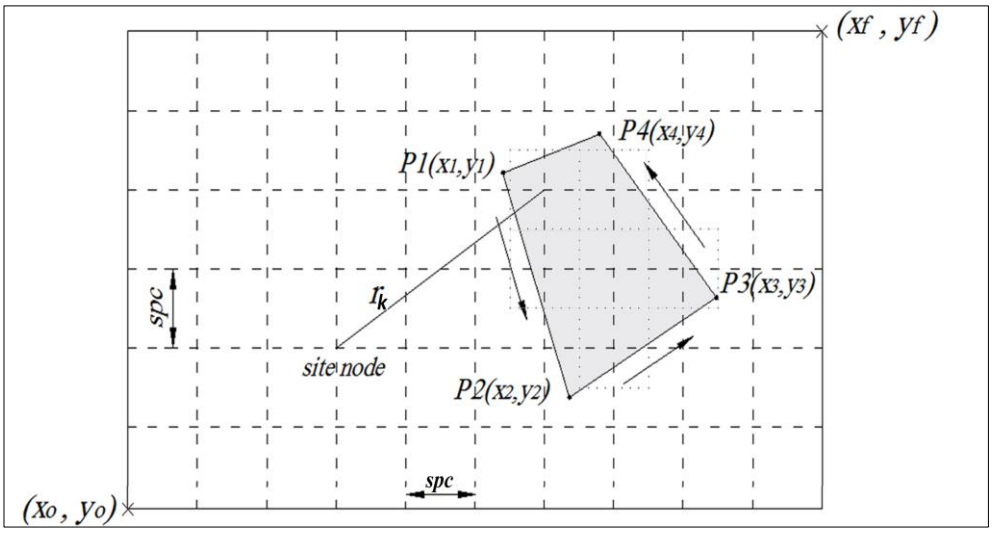

Figure 9. Identifying input method of study area and seismic sources

5.2. Identifying Earthquake Distances

After identifying and dividing each seismic source into the small elements, the distance from each node of the grid inside the source, (the geometric center of each element of the source), to any node of the grid within the study area, (the site), is considered as the epicentral distance, (r_{ek}), to that site. This distance will be computed from Equation 11 which will be used later in the GMPEs. Also, this distance is computed for each source element from its center to each grid node, (the site). Then, using spc equals 0.5°, the number of the nodes of the grid will be 899, therefore, this distance will be computed 899 times for each small element of the twelve seismic sources. Next, the area of each element will be computed from Equation 10, then the total area of each source will be computed by summation of areas of all elements

of the source. This is for using Equation 9 in computing $P(R_i = r_{ek})$ to be used later in the main Equation of the PSHA, (Equation 7).

5.3. Identifying Earthquake Magnitudes

Equations 12, 13 will be used to compute the discrete probability distribution of magnitudes for each seismic source. A magnitude increment of dm=0.1 will be used in Equation 13. In order to use Equation 12, the maximum expected magnitude, m_{max}, need to be computed or specified for each source. The method of Kijko and Singh (2011) to calculate m_{max} will be used, basing on the observed m_{max} from the instrumental and historical data. But, this solution needs the results of completeness analysis such as M_c, b, etc., of each source [30]. Therefore, the completeness analysis will be applied firstly, using the goodness of fit method, for each source [22]. Also, a minimum magnitude of 4.3 will be adopted for all sources. The activity parameters of all sources are presented in Table 1.

Table 1. The activity parameters of all seismic sources, (Mwmin = 4.3 for all sources)

Source Zone No.	Mc	G-R: *a*- value	G-R: *b*- value	Maximum expected Magnitude
1	4.8	5.6768	1.1824	7.65
2	4.4	4.9485	1.1835	7.50
3	4.0	3.0627	0.7896	7.35
4	4.7	2.2943	0.6776	7.35
5	4.9	5.7409	1.1873	7.05
6	4.6	5.9087	1.1152	7.42
7	4.9	5.2083	1.1146	7.20
8	4.9	4.9947	1.1922	5.97
9	4.6	4.9311	0.9927	7.79
10	4.1	3.2198	0.7783	7.42
11	4.2	3.2552	0.8294	6.75
12	4.3	3.1575	0.8554	5.75

5.4. Ground Motion Intensity

In case there is no available sufficient strong ground motion data, generally several numbers of ground motion prediction equations, (GMPEs), are selected, and then these equations are combined through a logic-tree approach [31]. The criteria mentioned by Cotton et al. (2006) includes many steps through which reasons should be found for rejecting equations and excluding them from the whole list of the available candidate equations [32].

Among the more general GMPEs developed worldwide, the European equations were built according to data sets of shallow crustal earthquakes which involve many records from the Middle Eastern countries like Turkey, Syria, Jordan, Iran, Algeria and Armenia. The majority of these countries are surrounding the boundaries of Iraq [33, 34]. This motivates using these equations as candidate models according to the criteria of Cotton et al. (2006) [32]. Further, and to ensure that there is no dependence or there is no overlap or the overlap is only partial in the data sets from which the GMPEs were generated, candidate equations that based on data sets of shallow crustal earthquakes that involve global records will be considered [6, 33]. Two GMPEs will be used for active regions which are that of [6, 34]. The two GMPEs of Pezeshk et al. (2015) and Al Noman et al. (2015) from NGA East project, (stable regions), will be used for the west stable region of Iraq. Also, the logic tree shown in Figure 10 summarizes the uncertainties in source characterization and GMPEs [35, 36].

5.5. Applying PSHA on Iraq

The soil type and the probability level (2%) were selected correspond to the requirements in recent Iraqi building codes. The PSHA computations were performed for PGA and spectral accelerations, (Sa), at periods of 0.2 and 1.0 seconds and for 2% probability of exceedance in a time interval of 50 years and 5% damping.

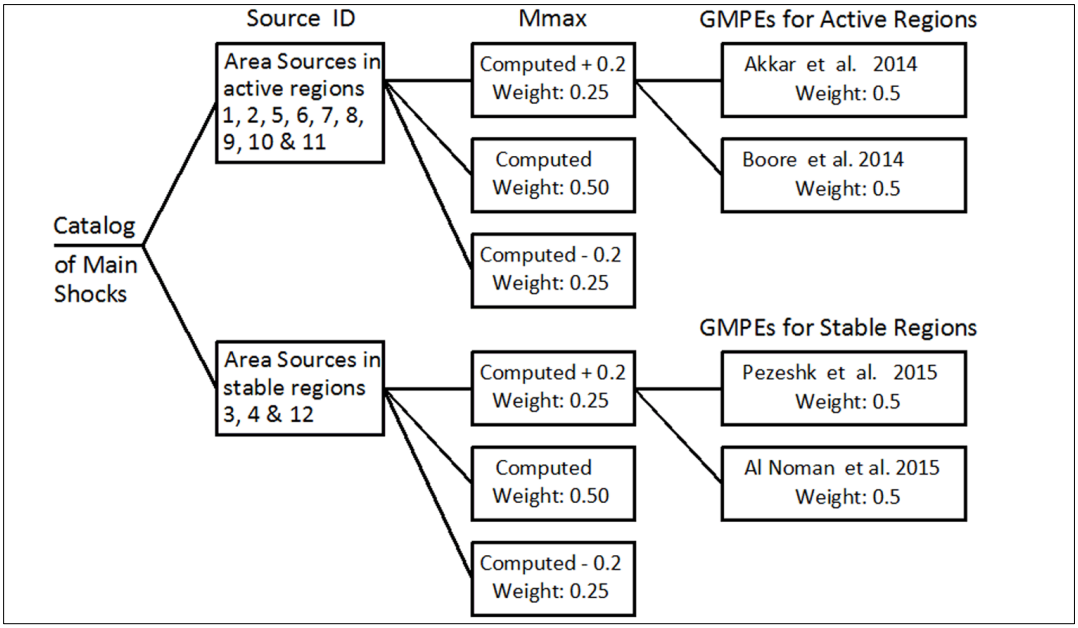

Figure 10. The Logic tree used in characterization of seismic sources and ground motion

The main program will solve Equations 7 and 14, which are the two main equations of PSHA, and applies a solving method deduced from the hazard curve principle to calculate the value of IM at each site. It begins by using IM values starting from the lowest value and then, iteratively increased by an equal increments. It can be seen from Figure 11 that as the value of IM increases, the probability of exceedance decreases and approaches 0.02 until it reaches 0.02 or a little less, in other word, the result of Equation 7 which is the value of $N(IM > x)$, becomes less than (1/2475). Now, the iteration process will be stopped, and the final value of IM is saved as the value at that node or site, and so on for other grid nodes. Hence, the output will be the values of PGA or Sa at a specified period and with a specified probability of exceedance and with a time interval of 50 years. This will be done at each site grid node, which means the output file will contain 899 of values for each IM, (acceleration), to be computed or for each run. Finally, the output file values are drawn as a contour map of Sa or PGA for the study region.

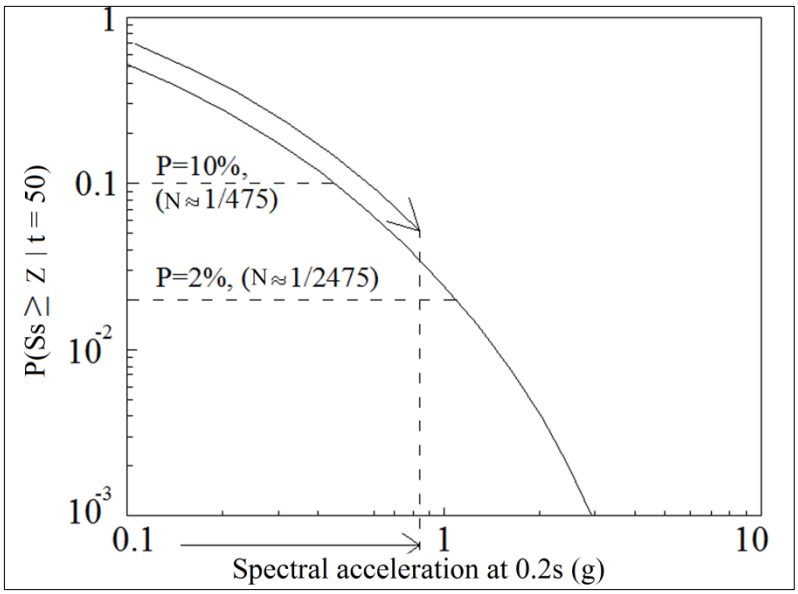

Figure 11. A simple example of a Hazard curve in terms of Ss

For the purpose of testing the work of the built program with other program or other work, it is necessary to mention that the seismic source model and the limits of the study area adopted in this study and then in the built program are the same as that adopted and used by Onur et al. (2016) and then, they used the software EqHaz. From this it can be deduced that if the same activity values, (Mmax, Mmin, b, a), are used, the results and then the work of the constructed program can be tested indirectly with the software EqHaz as compared to their results. This comparison is explained in Figure 12 in terms of Sa at 0.2 second. The comparison shows up the similarity in behavior and the values are very close especially in the boundary and interior of Iraq. There is a very small difference in values in a few places because of the difference in the used logic tree and used GMPEs. Figures 13, 14, 15 and 16 are the drawings of final results of this study. The

values increases towards the north and the east-northeast due to the continued tectonic boundary convergence between the Eurasian and Arabian plates which produces intense earthquake activity. From Figure 16, the design spectral accelerations at 0.2 and 1.0 secs. Equal 0.33, 0.17, 0.47, 0.25, 0.7 and 0.35 g for Basra, Baghdad and Erbil, respectively. Figure 17 was also drawn for comparison in Section (6).

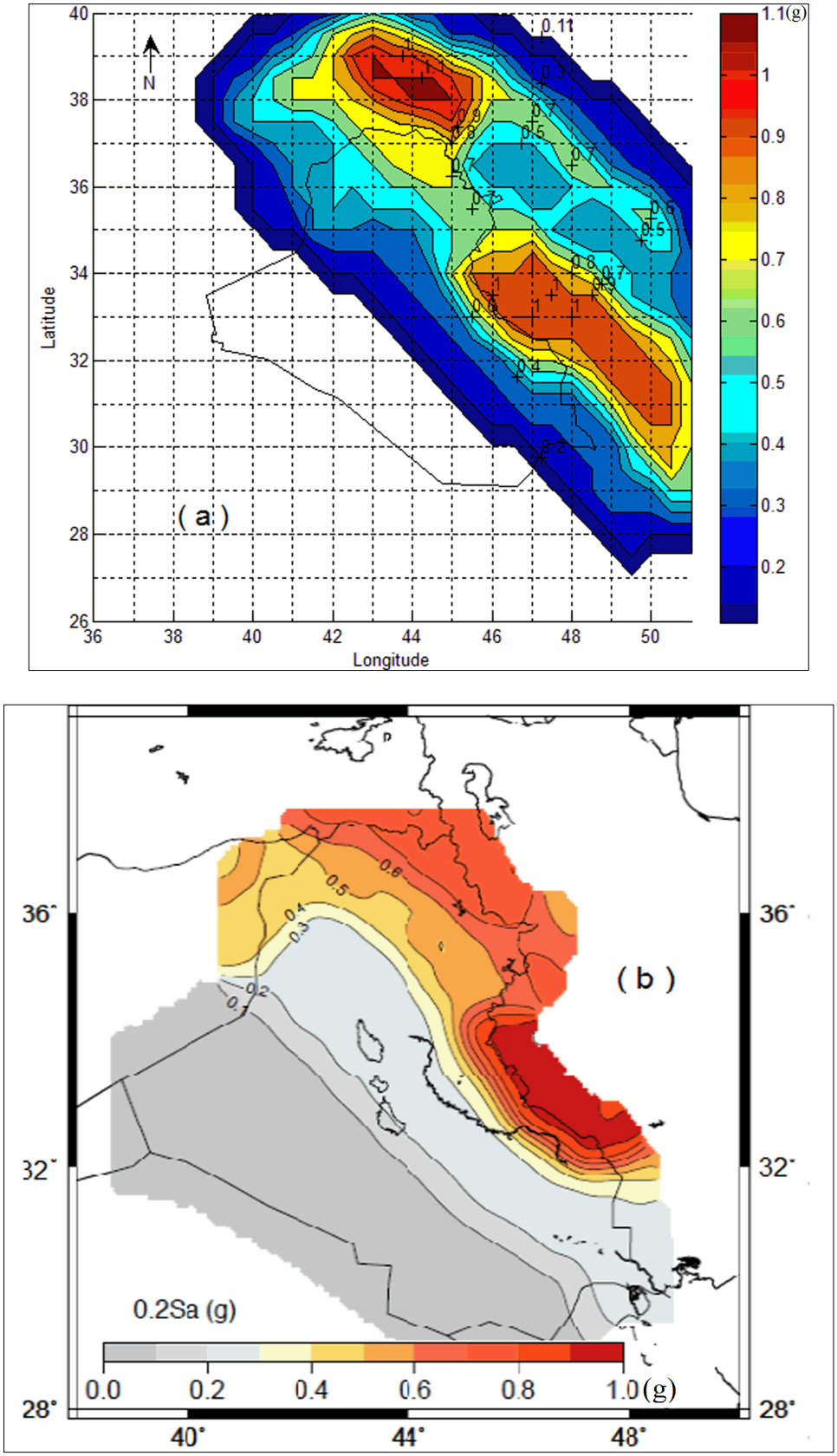

Figure 12. Spectral acceleration at 0.2 second for 2475 years return period on site class B, in units of (g), based on activity parameters (a, b, Mmin and Mmax) from Onur et al. (2016): a) Results of the constructed program of this study, b) Results of Onur et al. (2016)

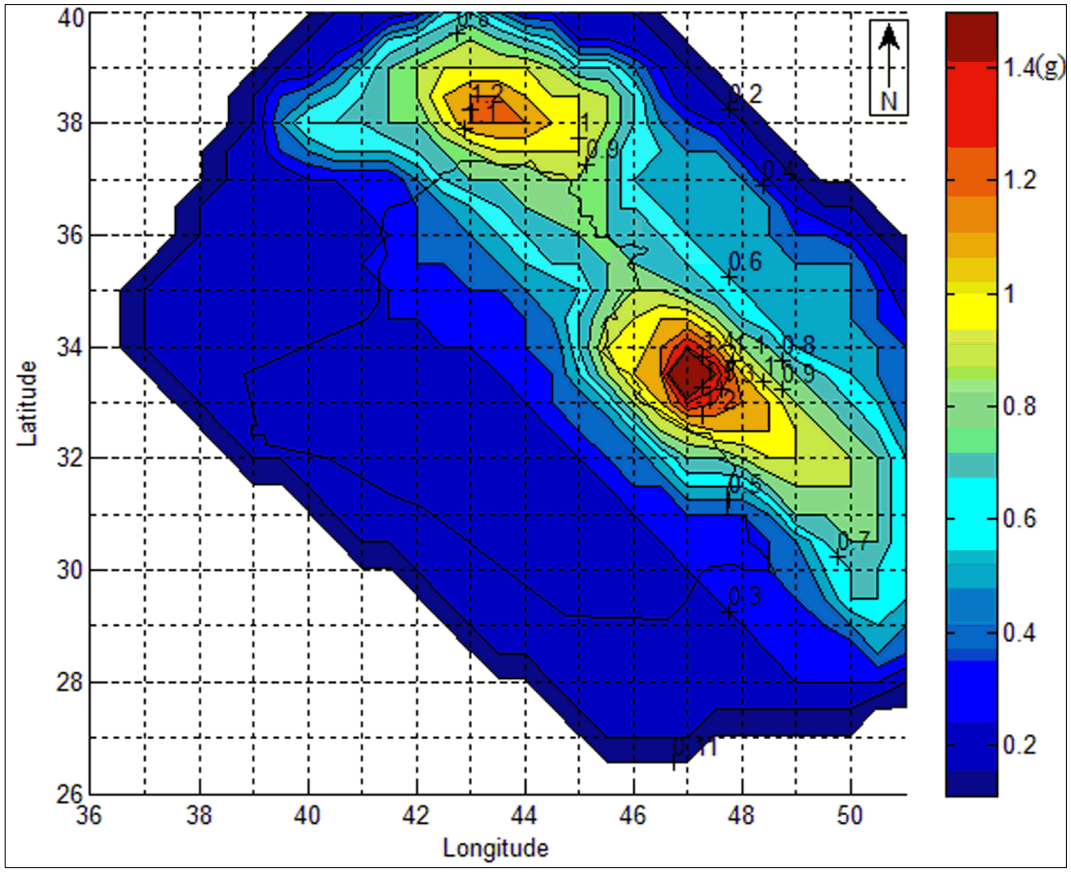

Figure 13. Spectral acceleration at 0.2sec for a return period of 2475 years on Site Class B, in units of (g)

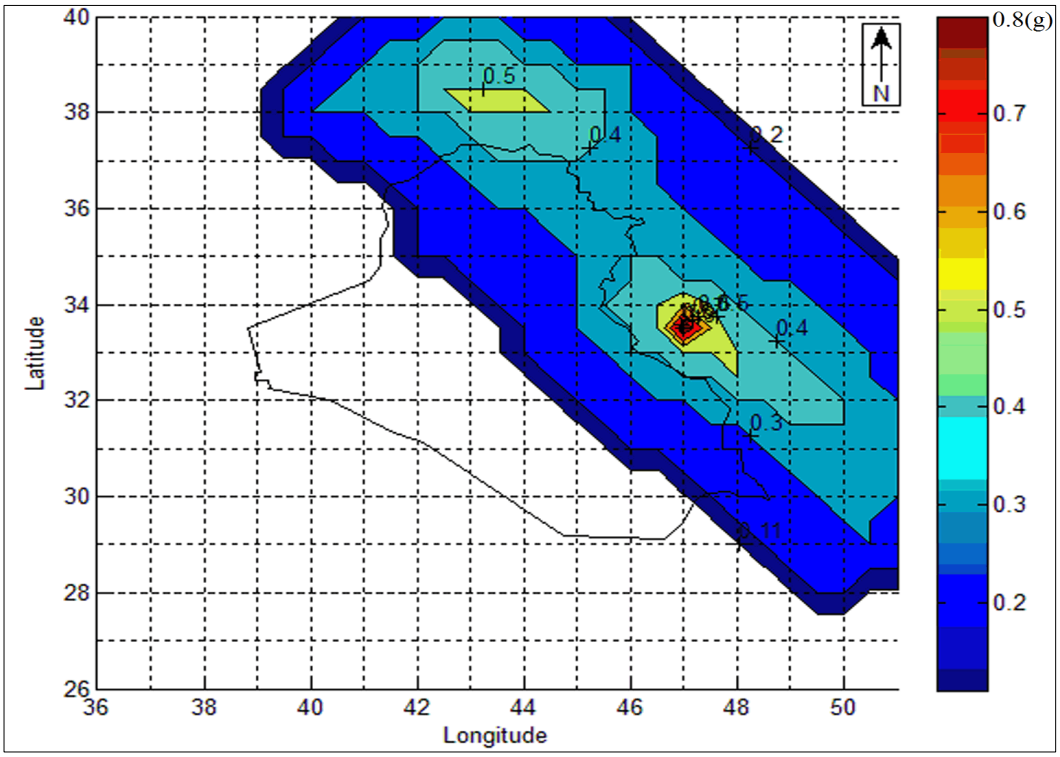

Figure 14. Spectral acceleration at 1.0 sec for a return period of 2475 years on Site Class B, in units of (g)

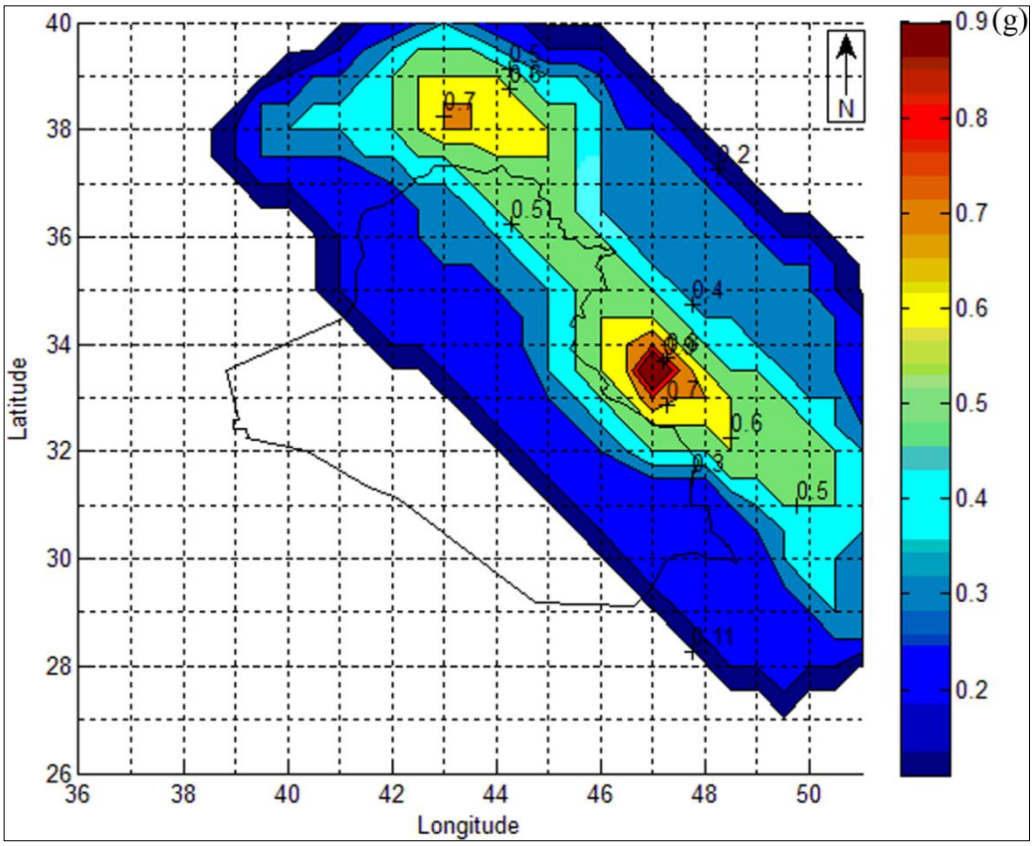

Figure 15. The peak ground acceleration for a return period of 2475 years on Site Class B, in units of (g)

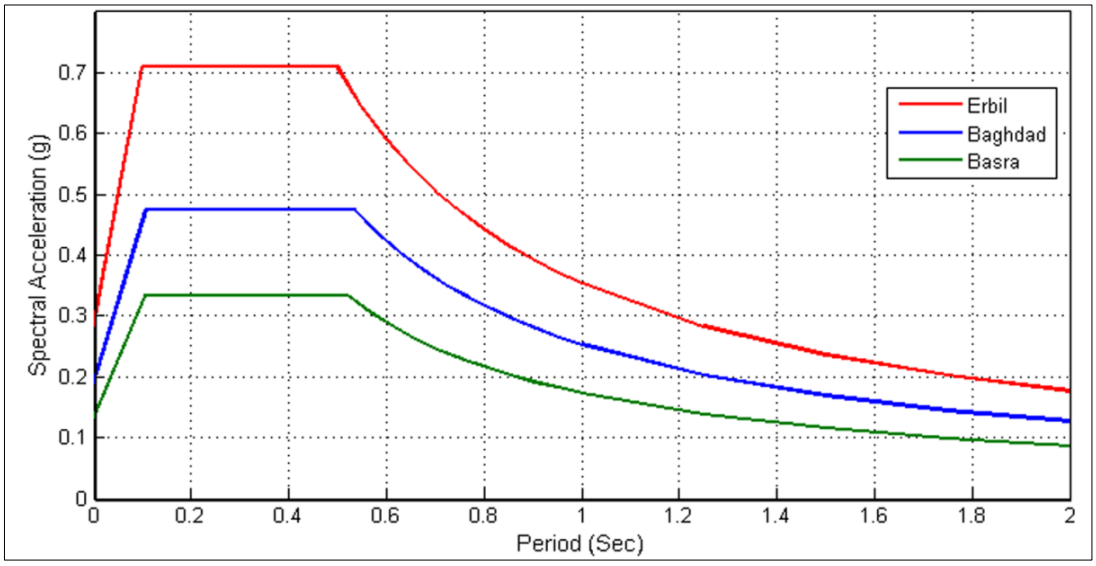

Figure 16. Design spectra for selected cities for a return period of 2475 years

6. Comparison with Values from the Seismic Design Code of Iraq

For comparison purpose, the PGA contour map for a return period of 475 years has also been plotted and then presented in Figure 17. The PGA values for the three main cities, (Baghdad, Basra and Erbil), were taken from Figure 17 and from seismic hazards maps of Iraq from Iraqi seismic code of 1989, 1997 and 2016 and they have been presented in Table 2 and then in Figure 18. The values of code 2016 have been transformed from a return period of 2475 years to a return period of 475 years by dividing on 1.71 according to the formula: PGA475= PGA2475*(10% / 2%)^(-1/3), (from Eurocode-8, section 2.1). Also, The PGA values for the three main cities were taken from figure 15 and from seismic hazards map of Iraq from Iraqi seismic code of 2016 for a return period of 2475 years, and they have been presented in Table 2 and then in Figure 19. It is worth mentioning that the seismic hazards maps of Iraq from Iraqi seismic code of 2016 is the same as that of Onur et al. (2016) which based on data of a period up to 2009. Also, the seismic hazards maps of Iraq from Iraqi seismic code of 1989 is based on data of a period up to 1986.

Generally, it can be seen that the PGA values increases for the three cities in each time period from 1986 to 1997, 1997 to 2009 and from 2009 to 2017 which reveals the need to updating the seismic hazard maps continuously.

It can be seen from figures 18 and 19 that the rate of increase in the PGA is largest in Basra and lowest in Erbil, while in Baghdad is in between. To interpret clearly this behavior although the largest earthquake has recently strike in the northeast boundary of Iraq with Iran, it is worth mentioning here that the PSHA method depend mainly on the probability of occurrence of earthquakes, namely, on the number of earthquakes and then on the intensity or magnitude of largest event. But, if the magnitude of the largest struck event is slightly larger than the magnitude of one of the previous ones, the number of earthquakes will be the dominant in affecting the results of the PSHA method. Thus, a simple statistical evaluation to the de-clustered seismic data adopted in this study revealed that the number of earthquakes within a circle of radius of 300 km around Basra, Baghdad and Erbil are 332, 176 and 124 events, respectively, as shown in Figure 20.

Thus, two points can be concluded from Figures 18 and 19, which are;

- The first is that from Figure 18, the rate of increase in the PGA in Basra increased in the period from 2009 to 2017 because the number of earthquakes has increased to such an extent that, despite the de-clustering process, the annual rate of occurrence of earthquakes has increased. While in Erbil is the opposite, where the rate of increase in the PGA is decreased in the period from 2009 to 2017 because the number of earthquakes due to the de-clustering process not increased to an extent that make the annual rate of earthquakes occurrence exceeds the rate in the previous periods. In Baghdad the case is in between, where the rate of increase in the PGA in the period from 2009 to 2017 is approximately the same as in previous periods.
- The second is that from Figures 18 and 19, the rate of increase in the PGA is largest in Basra and lower in Baghdad and the lowest in Erbil which is in agree with the number of earthquakes occurrences listed above within their surrounding circular regions, and as explained in Figure 20.

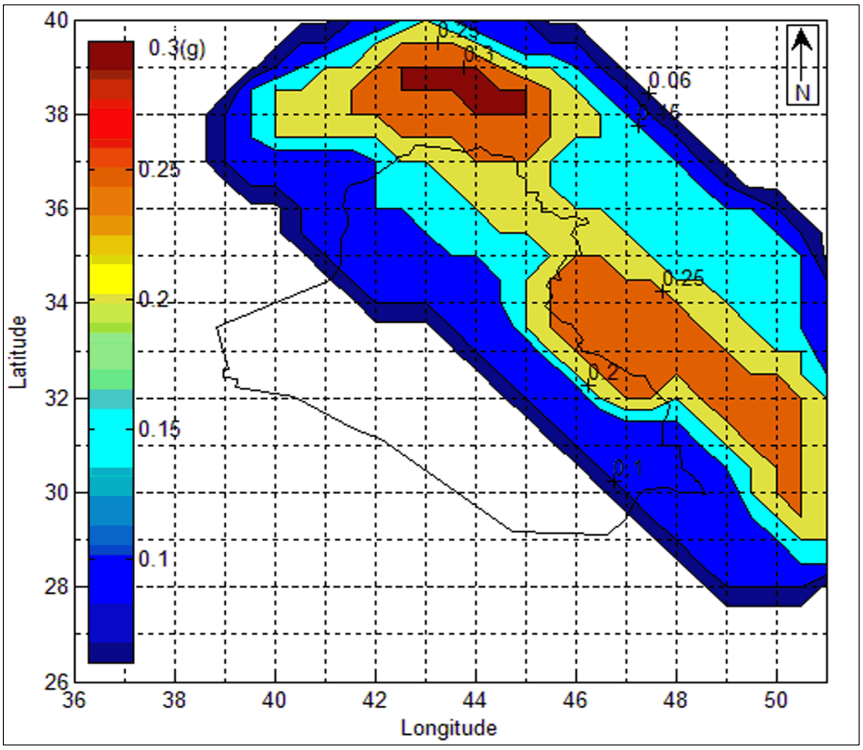

Figure 17. Peak ground acceleration (PGA) for a return period of 475 years on Site Class B, in units of (g)

Table 2. PGA values for return periods of 475 and 2475 years, on Site Class B, in units of (g)

Code	1989	1997	2016		This study	
Return period	475	475	2475	475	2475	475
Basra	0.025	0.05	0.125	0.073	0.25	0.12
Baghdad	0.045	0.05	0.175	0.102	0.28	0.14
Erbil	0.09	0.07	0.38	0.222	0.42	0.23

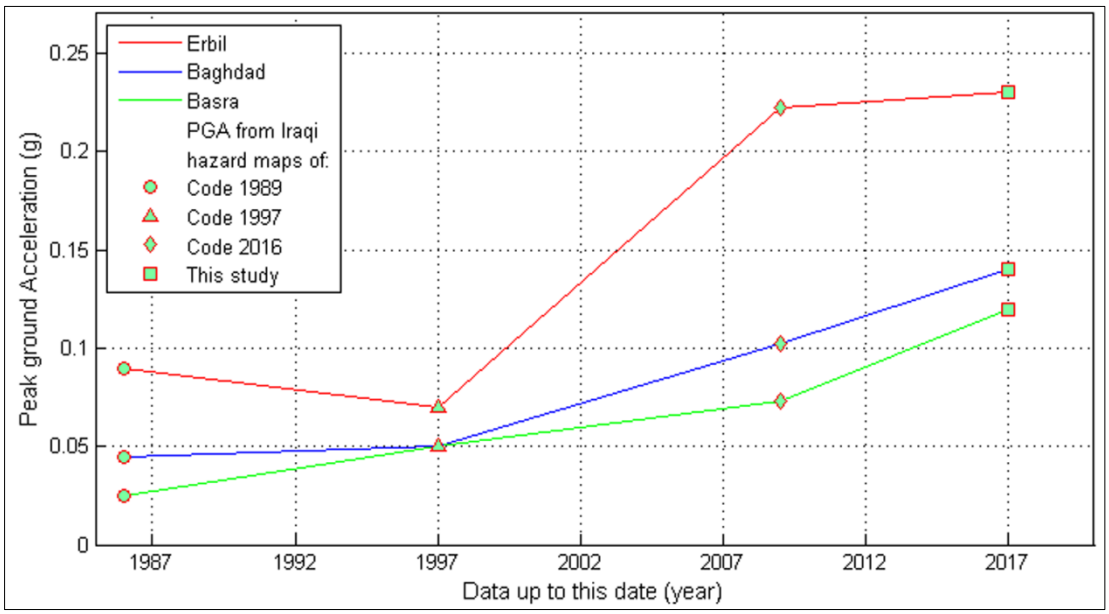

Figure 18. PGA values from the seismic design code of Iraq for versions (1989, 1997 and 2016) with that from this study for a return period of 475 years on site class B

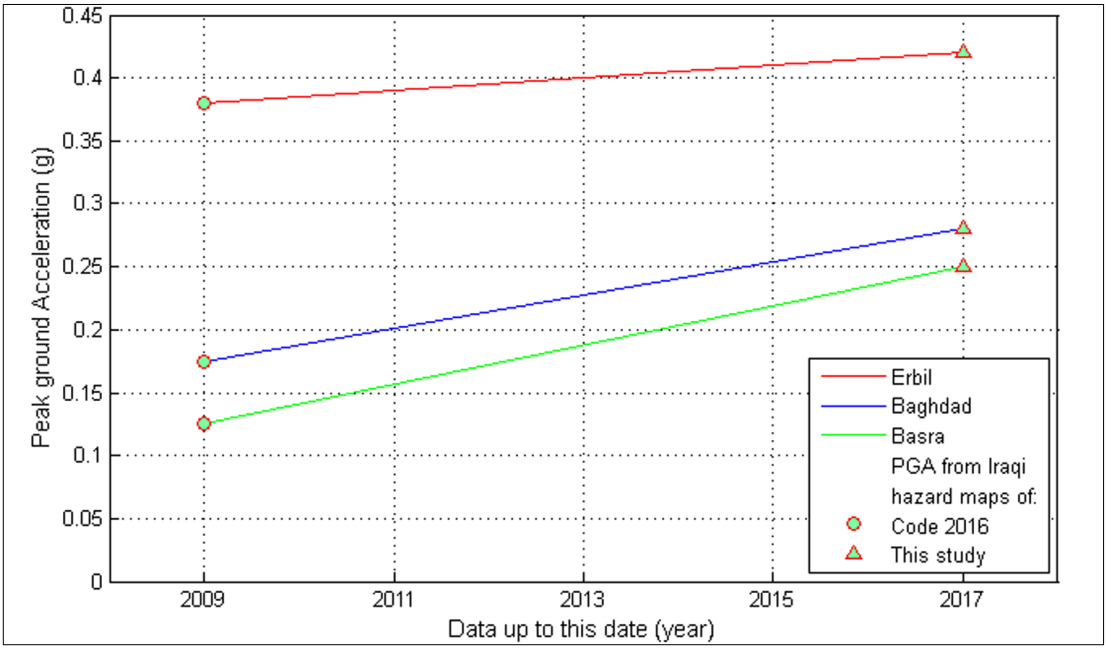

Figure 19. PGA values from the seismic design code of Iraq for version (2016) with that from this study for a return period of 2475 years on site class B

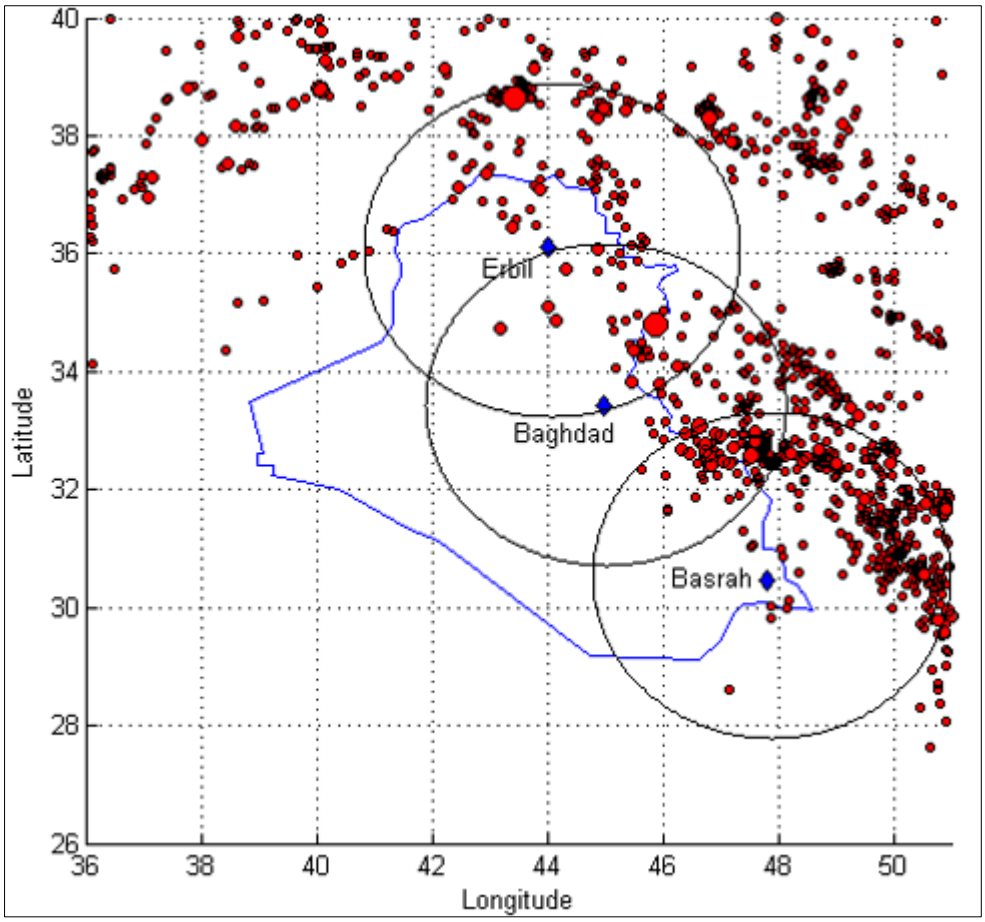

Figure 20. The earthquakes within a circles of radius of 300 km around each of Basra, Baghdad and Erbil

7. Conclusion

This paper presented a comprehensive study executed to prepare the seismic hazards maps of Iraq taking in to account the recently increased seismic activity. After removing duplicated events, de-clustering process has been applied on the resulted data which resulted in removing about 38% of them. Also, it is found that about 91% of the resulted main earthquakes have a depth ranging between 0 up to 35 km, which reveals that most of earthquakes in the Iraq territory exhibit shallow crustal seismic activity. Completeness analysis was performed on the de-clustered catalog for the whole region under study and then for each source zone. Completeness analysis results revealed that the data set of the de-clustered catalog were complete for Mw$\geqslant$5.4 since 1900 and it is found that the activity parameters are a= 6.4143 and b= 1.1114.

Also, completeness analysis was performed using the Stepp method, from which, the completeness intervals for the de-clustered catalog is found to be as following: 5.5<=Mw<6 are complete since 1900, 5.0<=Mw<5.5 since 1928, 4.5<= Mw<5 since 1968, 4.0<=Mw<4.5 since 1988. These findings have been fitted to GR law after preparing and extrapolating the recurrences of the previous completeness intervals along the total period. Thereafter from this fitting, it is found that the activity parameters are a=6.5681 and b=1.1327, which are near to that from Goodness of fit. Also, the built Matlab program, which used in PSHA analysis, has been tested and checked with other work and indirectly with EqHaz program. This comparison reveals good agreement in results.

The comparison between the PGA values from this study and from the seismic hazards maps from Iraqi seismic codes of 1989, 1997 and 2016, for return periods of 475 and 2475 years, reveals the continued increase with time which reveals the need to updating the seismic hazard maps continuously. Also, the rate of increase in the PGA in the period from the end of 2009 to the end of 2017 is largest in Basra and lower in Baghdad and the lowest in Erbil. The result of the PSHA method in this study presented in the form of contour maps of PGA and spectral accelerations at 0.2 second and 1.0 second. The values increases towards the north and the east-northeast due to the continued tectonic boundary convergence between the Eurasian and Arabian plates which produces intense earthquake activity. These contour maps were presented to be as an aid to prepare and construct the recent seismic hazard zoning maps of Iraq by rearranging and processing contour maps in such a way that they are divided into zones of Ss and zones of S1 values.

8. References

[1] Ghalib & Aleqabi/JZS. "Seismicity, Velocity Structure and Tectonics of the Arabian Plate." Journal of Zankoy Sulaimani 18 – 1 (Part-A) Pure and Applied Science (2016). doi.org/10.17656/jzs.10499

[2] Onur, T., Gök, R., Abdulnaby, W., Shakir, A.M., Mahdi, H., Numan, N.M.S., Al-Shukri, H., Chlaib, H.K., Ameen, T.H., Abd, N.A. (2016). "Probabilistic Seismic Hazard Assessment for Iraq." LLNL-691152.

[3] Ameer, A. S., Sharma, M. L., Wason, H. R., Alsinawi, S. A. (2005). "Probabilistic Seismic Hazard Assessment for Iraq Using Complete Earthquake Catalogue Files." Journal of Pure and Applied Geophysics 162 (2005): 951-966. Doi: 10.1007/s00024-004-2650-y

[4] Mahmood, D.S., Khalifa, S., Jordanovski, L., Dojcinovski, D. "Seismic hazard evaluation and seismic zoning maps of Iraq." Investigations for elaboration of preliminary seismic design code of Iraq, Building Research Center, Baghdad, Iraq, (1988).

[5] McGuire, R.K. "Seismic design spectra and mapping procedures using hazard analysis based directly on oscillator response." Earthquake Engineering and Structural Dynamics 5(3) (September 1977): 211-234. Doi: 10.1002/eqe.4290050302

[6] Esteva, L., Villaverde, R. "Seismic risk, design spectra and structural reliability." Proceedings of Fifth World Conference on Earthquake Engineering 2 (1973): 2586-2596.

[7] Fahmi, K.J., Alabbasi, J.N. "Seismic Intensity Zoning and Earthquake Risk Mapping in Iraq." Natural Hazards 1 (1988): 331 340. Doi: 10.1007/bf00134831.

[8] Cornell, C. A., Banon, H., Shakal, A. F. "Seismic motion and response prediction alternatives." Earthquake Engineering & Structural Dynamics 7 (1979): 295-315. Doi: 10.1002/eqe.4290070402.

[9] Al-Sinawi, S.A., Al-Qasrani, Z.O. "Earthquake Hazards Considerations for Iraq." Proc. 4rth Int. Conference of Earthquake Engineering and Seismology, Tehran, Iran. (May 2003).

[10] Boore, D. M., Stewart, J. P., Atkinson, G. M. (2014). "NGA-West2 Equations for Predicting PGA, PGV, and 5% Damped PSA for Shallow Crustal Earthquakes." Earthquake Spectra 30(3) (August 2014): 1057-1085. Doi: 10.1193/070113EQS184M.

[11] Chiou, B. S.-J., Youngs, R.R. "Update of the Chiou and Youngs NGA model for the average horizontal component of peak ground motion and response spectra." Earthquake Spectra 30(3) (August 2014): 1117-1153. Doi: 10.1193/072813EQS219M.

[12] Campbell, K.W., Bozorgnia, Y. "NGA-West2 Ground Motion Model for the Average Horizontal Components of PGA, PGV, and 5% Damped Linear Acceleration response spectra." Earthquake Spectra 30(3) (August 2014): 1087-1115. Doi: 10.1193/062913EQS175M.

[13] Yazdi, P., Zare, M. "Building an Earthquake Catalog for the Middle East." 15WCEE, LISBOA 2012, (2012).

[14] Scordilis, E.M. "Empirical global relations converting Ms and Mb to moment magnitude." Journal of Seismology 10 (January 2006): 225–236. Doi: 10.1007/s10950-006-9012-4.

[15] Wheeler, R. L. "Earthquakes of the Central United States, 1795-2002 – Construction of the earthquake catalog for an outreach map." U. S. Geological Survey, Open- File Report 03- 232, 14 P, (2003).

[16] Nasir, A., Lenhardt, W., Hintersberger, E., Decker, K. "Assessing the completeness of historical earthquake records in Austria and surrounding Central Europe." Austrian Journal of Earth Sciences 106/1 (2013): 90–102, Vienna.

[17] Gardner, J. K., Knopoff, L. (1974). "Is the sequence of earthquakes in Southern California, with aftershocks removed, Poissonian?." Bulletin of the Seismological Society of America Vol. 64, No. 5 (1974): 1363-1367.

[18] Knopoff, L. (2000). "The magnitude distribution of de-clustered earthquakes in Southern California." Proc. Natl. Acad. Sci. USA 97(22) (October 2000): 11880-11884. Doi: 10.1073/pnas.190241297.

[19] Uhrhammer, R. "Characteristics of Northern and Central California Seismicity." Earthquake Notes, 57(1) (1986): 21. Doi: 10.1785/gssrl.57.1.5.

[20] Van Stiphout, T., Zhuang, J., Marsan, D. "Seismicity De-clustering." (2012) Community Online Resource for Statistical Seismicity Analysis. Doi: 10.5078/corssa-52382934.

[21] Stepp, J.C. "Analysis of completeness of the earthquake sample in the Puget Sound area and its effect on statistical estimates of earthquake hazard." Proceedings of the International Conference on Microzonation, Seattle, U.S.A. 2 (1972): 897–910.

[22] Wiemer, S., Wyss, M. "Minimum Magnitude of Completeness in Earthquake Catalogs: Examples from Alaska, the Western United States, and Japan." Bulletin of the Seismological Society of America 90 (4) (August 2000): 859-869.Doi: 10.1785/0119990114.

[23] Gutenberg, B., Richter, C. F. "Frequency of earthquakes in California." Bulletin of the Seismological Society of America 34(4) (October 1944): 185-188.

[24] Baker, J. W. "An Introduction to Probabilistic Seismic Hazard Analysis (PSHA), Version 1.3." (October 2008).

[25] Cornell, C.A. "Engineering Seismic Risk Analysis." Bulletin of the Seismological Society of America 58(5) (October 1968): 1583–1606.

[26] Kramer, S.L. "Geotechnical earthquake engineering." Prentice-Hall International series in Civil Engineering and Engineering Mechanics, Upper Saddle River, N.J, (1996).

[27] Gupta, I. D. "Probabilistic Seismic Hazard Analysis method for mapping of spectral amplitudes and other design specific

quantities to estimate the earthquake effects on man-made structures." ISET Journal of Earthquake Technology, Paper No.480, 44(1) (March 2007): 127–167.

[28] Crowley, H., Damiano Monelli, Marco Pagani, Vitor Silva, Graeme Weatherill. "OpenQuake Book, Version 0.1." The GEM Foundation, Pavia, Italy, (September 2011).

[29] Gupta, I. D. "Source-to-site distance distributions for area type of seismic sources used in PSHA applications." Natural Hazards 66 (2013): 485–499. Doi: 10.1007/s11069-012-0498-5.

[30] Kijko, A., Singh, M. "Statistical Tools for Maximum Possible Earthquake Magnitude Estimation." Acta Geophysica 59 (4) (March 2011): 674-700. Doi: 10.2478/s11600-011-0012-6.

[31] Bommer, J.J., Scherbaum, F., Bungum, H., Cotton, F., Sabetta, F. "On the use of logic trees for ground-motion prediction equations in seismic hazard analysis." Bulletin of the Seismological Society of America 95(2) (April 2005): 377–389. Doi: 10.1785/0120040073.

[32] Cotton, F., Scherbaum, F., Bommer, J. J., Bungum, H. "Criteria for selecting and adjusting ground- motion models for specific target regions: Application to central Europe and rock sites." Journal of Seismology 10(2) (May 2006): 137-156. Doi: 10.1007/s10950-005-9006-7.

[33] Douglas, J. "Ground-motion prediction equations 1964–2016." (February 2017).

[34] Akkar, S., Sandikkaya, M. A., Bommer, J. J. (2014). "Empirical ground-motion models for point- and extended-source crustal earthquake scenarios in Europe and the Middle East." Bulletin of Earthquake Engineering (May 2013). Doi: 10.1007/s10518-013-9461-4.

[35] Pezeshk, S., Zandieh, A., Campbell, K.W., Tavakoli, B. "Ground-Motion Prediction Equations for CENA Using the Hybrid Empirical Method in Conjunction with NGA-West2 Empirical Ground-Motion Models. NGA-East: Median Ground-Motion Models for the Central and Eastern North America Region." PEER Report No. 2015/04 (April 2015): 119-147.

[36] Al Noman, Md. N., Cramer, C. H. "Empirical Ground-Motion Prediction Equations for Eastern North America. NGA-East: Median Ground-Motion Models for the Central and Eastern North America Region." PEER Report No.2015/04 (April 2015): 193-212.

[37] Iraqi Seismic Code Requirements for Buildings. Code 2/ 1997. Building Research Center, Baghdad, Iraq. https://www.scribd.com/document/256875867

[38] Iraqi Seismic Code Requirements for Buildings. Code 2016, 1st edition, C.O.S.Q.C., Baghdad, Iraq.